



## Computer simulation of radiation dose absorption in biological specimens

O.A. Kalatusha<sup>1,a</sup>, O.V. Ruban<sup>1</sup> and S.A. Nemnyugin<sup>1,b</sup>

<sup>1</sup> Saint-Petersburg University, 7/9 Universitetskaya nab., St.Petersburg, 199034, Russia

**e-mail:** <sup>a</sup> o.kalatusha@mail.spbu.ru, <sup>b</sup> s.nemnyugin@mail.spbu.ru

*Received 25 March 2016, in final form 12 April. Published 13 April 2016.*

**Abstract.** The radiation in biological tissues is considered. It is studied how the kind of a biological tissue determined by its chemical composition and physical characteristics, as well as the beam parameters, affect the radiation depth-dose distribution. Numerical results are obtained using the application using the software package Geant4. The results of our simulations may be used for better understanding of processes that play a crucial role in hadron therapy. The efficiency of hadron therapy is based on the Bragg peak phenomenon and more precise localization of the biological effect of a therapeutic beam.

**Keywords:** dose-depth distribution, radiation therapy, hadron therapy, Bragg peak, Monte-Carlo simulation

**MSC numbers:** 65C05, 92C50

## 1. Introduction

Beams of elementary particles and nuclei are widely used in many areas of technology, science, medicine etc. Therefore, the problems of accelerators design and the control of particles beams [1] are of significant importance. Understanding of the interaction of a particles beam with the target medium is also important from the practical point of view. Among the areas of application the design of radiation defence constructions for accelerators and space exploration systems should be mentioned.

The radiation therapy is an efficient method of the cancer treatment. Clinical practice shows that its efficiency in many cases exceeds 50% [2]. To improve the efficiency of radiation therapy it is necessary to deliver most of the radiation dose to the malignant tumor volume. At the same time, the surrounding tissues should obtain as little irradiation as possible. In conventional radiotherapy the beams of high-energy photons and light particles are used. The drawback of using the photons is that their energy deposition profiles have a wide smooth distribution under the surface of a specimen. So, if some deeply embedded tumor must be irradiated, healthy tissues will be also damaged.

The dependence of the absorbed dose upon the distance of a beam penetration for heavy charged particles (protons and heavy ions) has the form of a curve with the Bragg peak caused by sharp energy transfer at the end of the particle trajectory [3], [4], [5]. The biological effect of heavy charged particles is nearly the same as that of photons, but sharp localization of the dose absorbed improves the treatment efficiency [6], [7].

An important characteristic of the beam interaction with medium is its energy loss per unit path length (stopping power) or the linear energy transfer (LET):

$$L = \frac{dE}{dx}.$$

The theory of stopping power is under development for a long time [8], [9]. Analytical results have been obtained for the cases with simple target geometry and homogeneous medium, the target consisting of a single chemical element. The Bethe-Bloch formula defines  $L$  under such assumptions [10]:

$$\frac{1}{\rho}L = Kz^2 \frac{Z}{A} \frac{1}{\beta^2} \left[ \frac{1}{2} \ln \frac{2m_e c^2 \beta^2 \gamma^2 T_{max}}{I^2} - \beta^2 - \frac{\delta(\beta\gamma)}{2} \right],$$

where  $z$  is the charge of the incident particle,  $Z$  and  $A$  are the atomic number and mass of the target medium.  $I$  is the mean excitation energy of the target atom,  $\delta(\beta\gamma)$  is the density effect correction to the ionization energy loss,  $\beta$  and  $\gamma$  are relativistic factors.  $T_{max}$  is the maximum kinetic energy which may be delivered to a free electron in a single collision.

Due to a lot of processes which have to be taken into account, the complex chemical composition of biological tissues, the heterogeneity of the target, and the complicated static and dynamic geometries, the most reliable results may be obtained only by means of mathematical modelling and computer simulation methods.

At the same time the standard test case is a cube target filled by water or other homogeneous medium.

In the present paper the results of systematic study of LET profiles in biological tissues are presented. The treatment of deep-seated tumors requires ion beam energies up to nearly 200 MeV/u for protons and light ions, and 400 MeV/u for carbon ions. Within this range of energies LET is dominated by inelastic collisions with the target electrons. In our simulations the fragmentation of heavy ions was not taken into account. The fragmentation leads to the appearance of a small tail after the Bragg peak. Firstly, the computer simulation results were verified by comparison with the experimental data. Then the dose-depth distributions were calculated for mixtures of water and some chemical elements. The LET profiles were computed for biological tissues in uniform specimens. Dependencies of the Bragg peak characteristics on the beam parameters and the kind of biological tissue were derived from these results. The estimates of widening of the dose distribution broadening in the transverse plane were also obtained.

## 2. Computer simulation

Monte Carlo simulation methods are efficient methods of study of complex models when it is necessary to take a lot of processes, the complex geometry of a target and its heterogeneity into account. The simulation methods also may be used for testing the Treatment Planning Systems, in the process of developing hardware for centers of hadron therapy [11], [12], [13] etc. The Monte Carlo simulation may be time-consuming but it allows one to get the results with minimum of *a priori* approximations. The reliability of Monte Carlo simulation results was confirmed by many studies [14], [15].

There are software packages for Monte Carlo simulation which are based on semi-empirical models of the transport of elementary particles and ions in targets with any given geometry, physical properties and chemical composition. The most widely used packages are GEANT4 (GEometry And Tracking, 4th version) [16], Fluka (Fluktuerende Kaskade) [17], MCNPX (Monte Carlo N-Particle) [18] etc. We used Geant4.9.5 in our numerical studies.

GEANT4 is a set of libraries of C++ classes. The input data for modelling include [19]: the sort of particles, their mass, spin, energy, momentum and polarization, the beam characteristics, and the set of physical processes which have to be taken into account. The geometry, physical properties and chemical composition of the target also should be given. Geant4 allows getting detailed information about the interactions of primary and secondary particles with the medium.

The targets with pure water are used in radiation therapy as a reference for the sake of comparison with the results for biological tissues (soft, adipose, bones, lung and glands tissues). The chemical composition of biological tissues is defined according to standards of the Committee on Medical Internal Radiation Dose (MIRD) of the Society of Nuclear Medicine and Molecular Imaging, where the method of calculating the absorbed doses for internal human organs was developed [20].

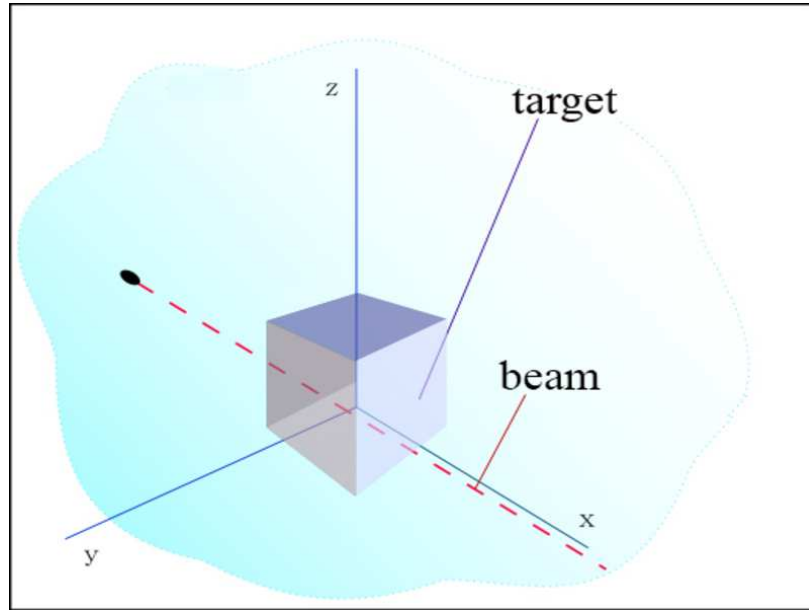


Figure 1: Geometry of the computational experiment.

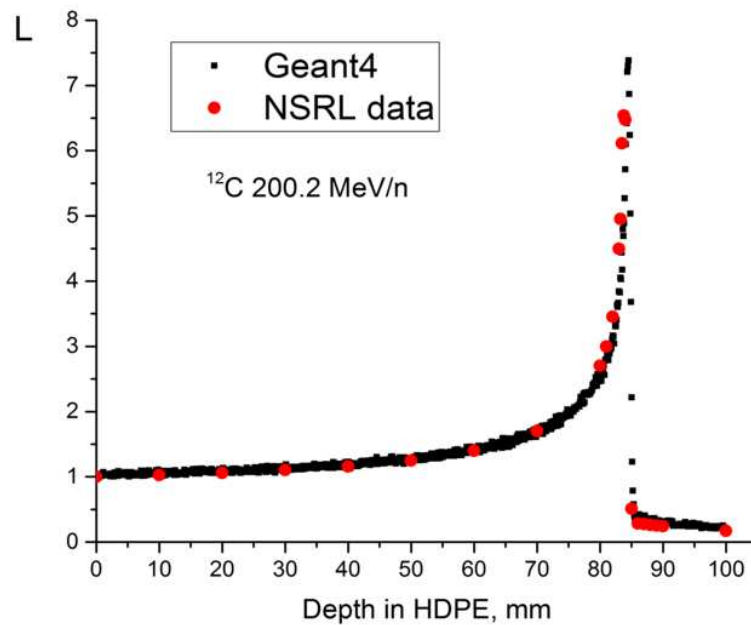


Figure 2: Comparison of experimental (dots) and computed (squares) dose-depth distributions for the carbon ion ( $^{12}\text{C}$ ) beam with energy 200.2 MeV/n in HDPE.

The geometry of the simulated experiment is presented in Fig. 1. The target is cube with the side length of 10 centimeters.

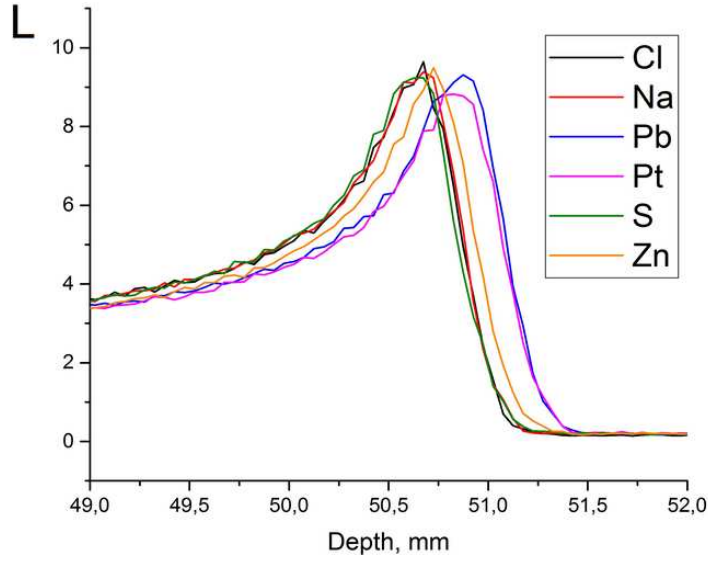


Figure 3: The absorbed dose distribution in a mixture of water and chemical elements for the carbon ion ( $^{12}\text{C}$ ) beam with energy 150 MeV/n.

Table 1: Chemical composition and density of biological tissues

	Adipose	Gland	Lung	Bone	Soft
<b>Density,</b> $g/cm^3$	0.93	1.04	0.2958	1.4862	0.9869
<b>H</b>	$1.12 \times 10^{-1}$	$1.0 \times 10^{-1}$	$1.021 \times 10^{-1}$	$7.04 \times 10^{-2}$	$1.047 \times 10^{-1}$
<b>C</b>	$6.19 \times 10^{-1}$	$1.84 \times 10^{-1}$	$1.001 \times 10^{-1}$	$2.279 \times 10^{-1}$	$2.302 \times 10^{-1}$
<b>N</b>	$1.7 \times 10^{-2}$	$3.2 \times 10^{-2}$	$2.8 \times 10^{-2}$	$3.87 \times 10^{-2}$	$2.34 \times 10^{-2}$
<b>O</b>	$2.51 \times 10^{-1}$	$6.79 \times 10^{-1}$	$7.596 \times 10^{-1}$	$4.856 \times 10^{-1}$	$6.321 \times 10^{-1}$
<b>Na</b>	-	-	$1.9 \times 10^{-3}$	$3.2 \times 10^{-3}$	$1.3 \times 10^{-3}$
<b>Mg</b>	-	-	$7.4 \times 10^{-5}$	$1.1 \times 10^{-3}$	$1.5 \times 10^{-4}$
<b>P</b>	$2.5 \times 10^{-4}$	$1.25 \times 10^{-3}$	$8.1 \times 10^{-4}$	$6.94 \times 10^{-2}$	$2.4 \times 10^{-2}$
<b>S</b>	$2.5 \times 10^{-4}$	$1.25 \times 10^{-3}$	$2.3 \times 10^{-3}$	$1.7 \times 10^{-3}$	$2.2 \times 10^{-3}$
<b>Cl</b>	-	-	$2.7 \times 10^{-3}$	$1.4 \times 10^{-3}$	$1.4 \times 10^{-3}$
<b>K</b>	$2.5 \times 10^{-4}$	$1.25 \times 10^{-3}$	$2.0 \times 10^{-3}$	$1.5 \times 10^{-3}$	$2.1 \times 10^{-3}$
<b>Fe</b>	-	-	$3.7 \times 10^{-4}$	$8.0 \times 10^{-5}$	$6.3 \times 10^{-5}$
<b>Zn</b>	-	-	$1.1 \times 10^{-5}$	$4.8 \times 10^{-5}$	$3.2 \times 10^{-5}$
<b>Rb</b>	-	-	$3.7 \times 10^{-6}$	-	$5.7 \times 10^{-6}$
<b>Sr</b>	-	-	$5.9 \times 10^{-8}$	$3.2 \times 10^{-5}$	$3.4 \times 10^{-7}$
<b>Zr</b>	-	-	-	-	$0.8 \times 10^{-5}$
<b>Pb</b>	-	-	$4.1 \times 10^{-7}$	$1.1 \times 10^{-5}$	$1.6 \times 10^{-7}$
<b>Ca</b>	$2.5 \times 10^{-4}$	$1.25 \times 10^{-3}$	$7.0 \times 10^{-5}$	$9.91 \times 10^{-2}$	-

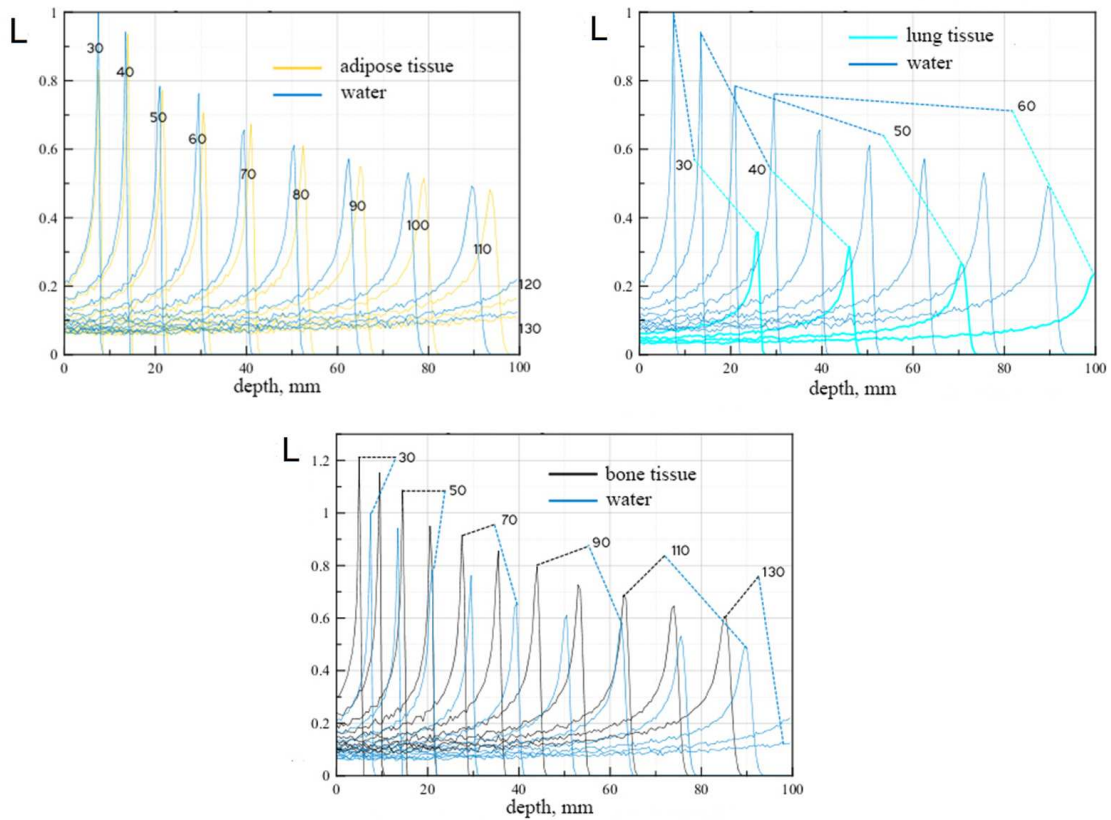


Figure 4: The absorbed dose distribution in water, adipose, lung and bone tissues for the proton beams with different energies.

The comparison of the numerical results with the experimental data from the NASA Space Radiation Laboratory for HDPE, the high-density polyethylene [21], is presented in Fig. 2. The Bragg peak is reproduced and the agreement of simulation results with experimental data is good. It confirms the correctness of the physical model used in our calculations.

$L$  was computed for mixtures of water and chemical elements (Cl, Na, Pb, Pt, S and Zn), which are constituents of biological tissues or medicines used in chemotherapy. The target cube is filled by the homogeneous mixture of water and 15 milligrams of a chemical element. The sample size in Monte Carlo simulations corresponds to the irradiation of the target by 1000 carbon ions. The beam energy is 150 MeV per nucleon. This value is in the medical interval of beam energies. The plots of the absorbed doses are presented in Fig. 3.

It is seen from Fig. 3 that the Bragg peak position depends on the atomic number of the admixture. The depth of the Bragg peak localization is greater for heavier elements.

In the simulations of beam interaction with biological tissues the target cube is filled by a homogeneous medium. The sample size corresponds to 10000 protons. The chemical composition of tissues is given in Table 1. Any tissue is considered as a simple mixture of chemical elements.

### 3. LET profiles in biological tissues

The results of the computation of LET profiles for water, adiposis, lung and bone tissues are presented in Fig. 4. The proton beams were considered with the energies from 10 to 130 MeV changing with the step equal to 10 MeV.

The Bragg peak is characterized by its distance from the target surface, the energy in the maximum and the width of the peak at half-maximum level. It is seen from Fig. 5 that the difference of peak positions in the tissue and pure water increases when the depth of localization increases. The difference is significant in the length scale of a human body. For less dense media such as the lung tissue, the shift is positive and for denser medium (the bone tissue for example) it is negative.

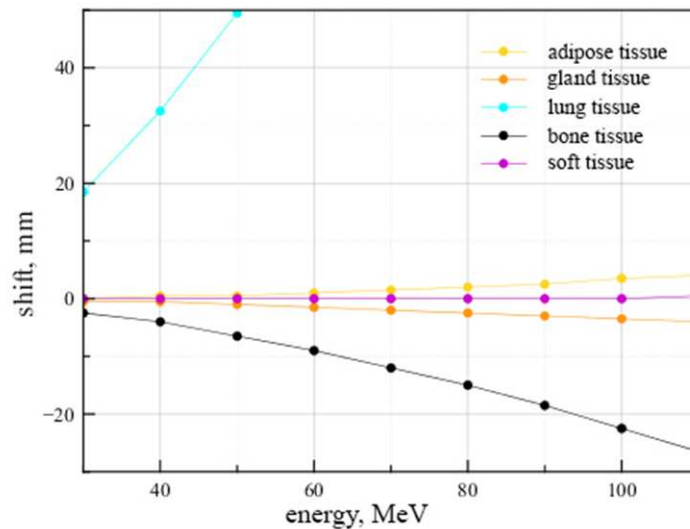


Figure 5: The difference of the Bragg peak position in biological tissues and water for the proton beams with different energies.

The width of the Bragg peak characterizes the precision of the dose deposition in a target. The results of our simulations (see Fig. 6) demonstrate that the peak width decreases in denser medium. It also depends on the energy of the incident beam and increases for higher energies. As to the height of the Bragg peak, it goes down when the beam energy increases.

We also studied the transverse widening of the Bragg peak in the plane, perpendicular to the beam direction. In Fig. 7 (left) the transverse broadening of Bragg peaks in water is shown for the set of initial energy values of a proton beam. In Fig. 7 (right) the transverse broadening of the Bragg peak in water, lung and bone tissues is displayed. It is seen that the transverse broadening is nearly the same for the tissues with different densities. It depends only on the energy of the proton beam.

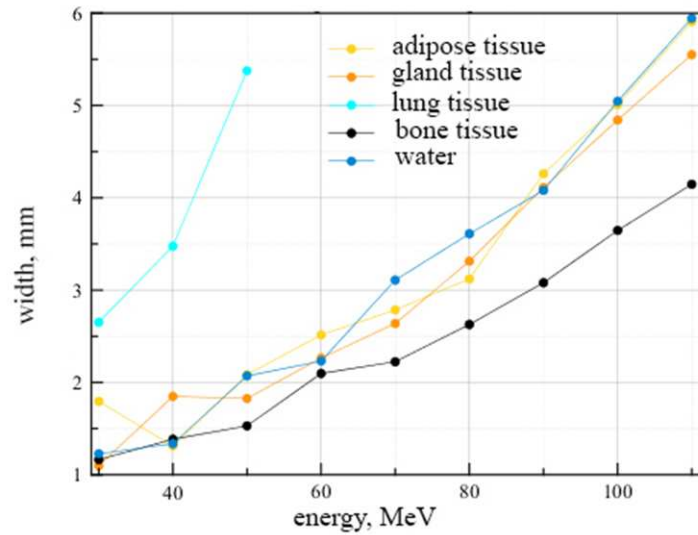


Figure 6: The width of the Bragg peak in biological tissues and water for the proton beams with different energies.

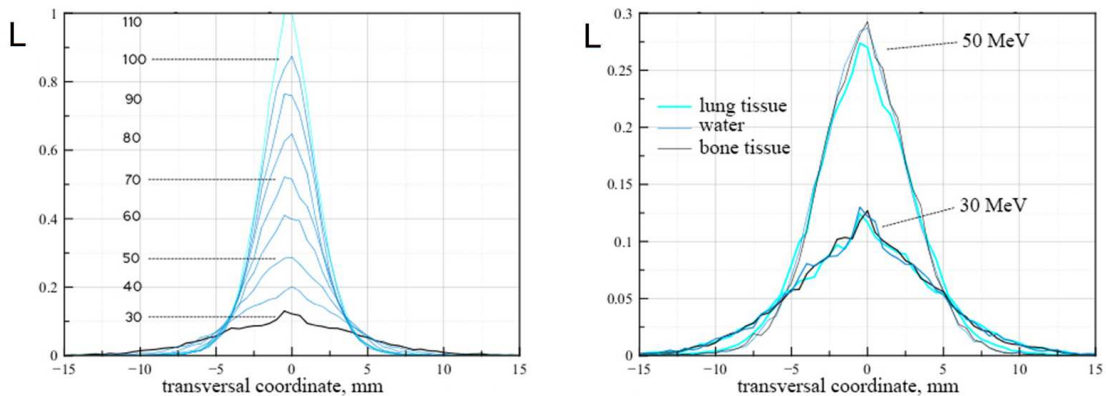


Figure 7: Transverse LET profiles in water (left) and tissues (right) for the proton beams with different energies.

## 4. Conclusion

Computer simulation study of interactions between proton beams and different kinds of media including biological tissues was performed using the application developed in the environment of the Geant4 software package. The plots of absorbed radiation doses versus penetration depth demonstrate the Bragg peak and agree with the experimental data. The main attention in our study was focused on how the kind of medium, its chemical composition, and the characteristics of the beam affect the depth of the Bragg peak localization and its width. The results for the pure water target and targets filled with simple mixtures of water with different



chemical elements are obtained. The systematic study of proton beams interaction with biological tissues is also performed. It was observed how the energy of the incident beam and the kind of biological tissue affect the depth of the Bragg peak localization and its width both in the beam direction and in the transverse plane. These results may be used for improving the efficiency of treatment planning in hadron therapy. In more realistic models non-uniformity of chemical composition and physical properties of biological tissues inside the human body should be taken into account.

## References

- [1] Malafeyev, O.A., Nemnyugin, S.A., Alferov, G.V. *Charged particles beam focusing with uncontrollable changing parameters.* // 2014 Tenth IVESC and Second International Conference on Emission Electronics ICEE / Proceedings edited by N. V. Egorov. Piscataway: IEEE, 2014. P. 25.
- [2] Shardt D. and Elsasser T. *Heavy-ion tumor therapy: Physical and radiobiological benefits.* Rev. Mod. Phys., 2010, **82**, pp.383-425.
- [3] Bragg W. *On the  $\alpha$ -particles of radium and their loss of range in passing through various atoms and molecules.* Philos. Mag., 1905, **10**, pp.318-340.
- [4] Jones B. *The Potential Clinical Advantages of Charged Particle Radiotherapy using Protons or Light Ions.* Clinical Oncology, 2008, **20**, pp.555-563.
- [5] Wilson R. *Radiological use of fast protons.* Radiology, Ed. by Radiological Society of North America, 1946, pp.487-491.
- [6] Chu William T. *Overview of Light-Ion Beam Therapy.* Paper LBNL, 2006, pp.21.
- [7] Khoroshkov V. S. *Radiation Beam Therapy Evolution: From X-rays to Hadrons.* Physics of Atomic Nuclei, 2006, **69**, pp.1724-1742.
- [8] Fano, U. *Penetration of protons, alpha particles and mesons.* Annu. Rev. Nucl. Sci., 1963, **13**, pp.1-66.
- [9] Ziegler J. F. et al. *SRIM — The Stopping and Range of Ions in Matter.* 2008.
- [10] Croom D.E. and Klein S.R. *Passage of particles through matter.* Eur. Phys. J., 2000, **C 15** (1-4), pp.163–173.
- [11] Newhauser W. et al. *Monte Carlo simulations for configuring and testing an analytical proton dose-calculation algorithm.* Phys. Med. Biol., 2007, **52**, pp.4569-4584.

- 
- [12] Fontenot J. et al. *Equivalent dose and effective dose from stray radiation during passively scattered proton radiotherapy for prostate cancer*. Phys. Med. Biol., 2008, **53**, pp. 1677-1688.
- [13] Titt U. and Newhauser W. D., *Neutron shielding calculations in a proton therapy facility based on Monte Carlo simulations and analytical models: Criterion for selecting the method of choice*. Radiat. Prot. Dosim., 2005, **115**, pp. 144-148.
- [14] Titt U. et al. *Assessment of the accuracy of an MCNPX-based Monte Carlo simulation model for predicting three-dimensional absorbed dose distributions*. Phys. Med. Biol., 2008, **53**, pp. 4455-4470.
- [15] Schaffner B. et al. *Dose calculation models for proton treatment planning using a dynamic beam delivery system: An attempt to include density heterogeneity effects in the analytical dose calculation*. Phys. Med. Biol., 1999, **44**, pp. 27-41.
- [16] [Web site of the GEANT project.](#)
- [17] [Web site of the Fluka project.](#)
- [18] [Web site of the MCNPX project.](#)
- [19] [Geant4 User's Guide. For Application Developers.](#)
- [20] Snyder W.S. et al. *MIRD Pamphlet No. 5 Revised, Estimates of absorbed fractions for monoenergetic photon sources uniformly distributed in various organs of a heterogeneous phantom*, J. Nucl. Med. Suppl., 1969, **3**, pp. 5-52.
- [21] [NASA Space Radiation Laboratory. User Guide. Technical data.](#)